Micromachines **2015**, *6*, 1346-1364; doi:10.3390/mi6091346

OPEN ACCESS

micromachines

ISSN 2072-666X

www.mdpi.com/journal/micromachines

Review

Magnetic Actuation Based Motion Control for Microrobots: An Overview

Tiantian Xu [1,2,*], Jiangfan Yu [1], Xiaohui Yan [1], Hongsoo Choi [3,*] and Li Zhang [1,2,4,*]

[1] Department of Mechanical and Automation Engineering, The Chinese University of Hong Kong, Shatin, Hong Kong, China; E-Mails: jeffyujf@gmail.com (J.Y.); xhyan@mae.cuhk.edu.hk (X.Y.)

[2] Shenzhen Research Institute, The Chinese University of Hong Kong, Shenzhen 518100, China

[3] Robotics Engineering Department, Daegu Gyeongbuk Institute of Science and Technology (DGIST), Daegu 704-230, Korea

[4] Chow Yuk Ho Technology Centre for Innovative Medicine, The Chinese University of Hong Kong, Shatin, Hong Kong, China

* Authors to whom correspondence should be addressed; E-Mails: ttxu@mae.cuhk.edu.hk (T.X.); mems@dgist.ac.kr (H.C.); lizhang@mae.cuhk.edu.hk (L.Z.); Tel.: +852-3943-1150 (T.X. & L.Z.); +82-53-785-6212 (H.C.).

Academic Editors: Toshio Fukuda, Mohd Ridzuan bin Ahmad and Yajing Shen

Received: 21 July 2015 / Accepted: 9 September 2015 / Published: 15 September 2015

Abstract: Untethered, controllable, mobile microrobots have been proposed for numerous applications, ranging from micro-manipulation, *in vitro* tasks (e.g., operation of microscale biological substances) to *in vivo* applications (e.g., targeted drug delivery; brachytherapy; hyperthermia, *etc*.), due to their small-scale dimensions and accessibility to tiny and complex environments. Researchers have used different magnetic actuation systems allowing custom-designed workspace and multiple degrees of freedom (DoF) to actuate microrobots with various motion control methods from open-loop pre-programmed control to closed-loop path-following control. This article provides an overview of the magnetic actuation systems and the magnetic actuation-based control methods for microrobots. An overall benchmark on the magnetic actuation system and control method is also discussed according to the applications of microrobots.

Keywords: microrobots; magnetic actuation; control

---

1. Introduction

Untethered, controllable, mobile microrobots have been proposed for numerous applications, ranging from industrial tasks, *in vitro* tasks to *in vivo* applications, due to their small-scale dimensions and accessibility to tiny and complex environments [1–9]. Industrial tasks include micro-manipulation, transporting and sorting of micro-objects, which enables robotic micro-assembly [10–12]. Microrobots are promising tools for interactions with biological cells, such as applications for cell surgery, because of their high throughput and high repeatability. Indeed, microrobots can operate down to the cellular or sub-cellular scale, allowing efficient *in vitro* interactions in order to move and sort cells [13–15]. Integration of a microfluidic chip and robotics based on micro-electromechanical (MEMS) systems technology is an innovation for biomedicine [16–18]. Accurate motion control, high propulsion power and the pumping mechanism of motion permit the microrobot to load multiple objects and transport them to desired locations in the microfluidic chip [19,20]. Microrobots present also opportunities for a wide range of environmental applications, such as environmental sensing, monitoring and remediation [21]. *In vivo* applications of microrobots are especially applied in minimally-invasive surgery, including [4,22–25]: targeted drug delivery, brachytherapy, hyperthermia, removing material by mechanical means or acting as simple static structures. Some locations in the human body would become available for wireless intervention, including the circulatory system, the urinary system and the central nervous system, if we were able to create microrobots with a maximum dimension of only a few millimeters or less. Microrobots will undoubtedly lead to the development of therapies.

Powering microrobots through built-in energy sources is currently hard to implement, due to the size of microrobots. Therefore, several off-board actuation methods have been used, such as the actuation of a microscale dielectric particle by dielectrophoresis forces generated by an electric field [26], piezo-electric actuation [27], thermal actuation [28], propulsion by electro-osmotic force [29], actuation by biological bacteria [30,31] and chemical fuel-driven micro-motors [32,33]. All of the above methods have some challenges, in particular for practical applications *in vivo*, for example piezo-electric actuation requires high voltages, and actuation by bacteria requires maintaining low cytotoxicity. Alternatively, magnetic fields can also be used as a transmitted power source, in which the forces and torques generated by magnetic fields can be applied without any perturbation by the bio-chemical fluids [34]. In this article, we focus on the magnetic actuation-based motion control of microrobots. In the literature, swimming microrobots are wirelessly propelled in a fluid environment: some of them can be pulled by a magnetic gradient [35]; some of them having helical structures are rotated by a rotating magnetic field and convert the rotation to linear displacement [36–39]. Researchers have used different magnetic actuation systems allowing differently-sized workspace and degrees of freedom (DoF). Various motion control methods have been applied, developing from open-loop control [36,37,40,41] to closed-loop point-to-point positioning control [35,42] or closed-loop path following [43]. The aim of this paper is to review the magnetic actuation systems and the motion control methods for microrobots. An overall benchmark on the magnetic actuation systems and control method according to the applications will also be discussed.

This paper is organized as follows: Section 2 presents the magnetic actuation by magnetic forces and torques; Section 3 reviews the various magnetic actuation systems allowing differently-sized workspace

and DoF; the motion control methods from open-loop pre-programmed control to closed-loop path following are reviewed in Section 4; the discussion of the choice of magnetic the actuation system and motion control method is included in Section 5, with a conclusion and the challenges for futures works.

2. Magnetic Actuation: Forces and Torques

The principle of magnetic actuation is to propel microrobots with magnetic forces and/or torques. A quasi-static and low-frequency magnetic field is an approach to apply forces and torques directly to magnetic materials without the need for any tethers or direct contact [4]. Magnetized objects can be exerted forces and torques within an externally-imposed magnetic field. The magnetic forces and torques developed on a magnetized object are expressed as follows [44]:

$$\overrightarrow{f_m} = \int_{V_m} (\overrightarrow{m} \cdot \bigtriangledown) \overrightarrow{B} \, dV_m \tag{1}$$

$$\overrightarrow{\tau_m} = \int_{V_m} \overrightarrow{m} \times \overrightarrow{B} \, dV_m \tag{2}$$

where V_m is the volume of the magnetized object, $\overrightarrow{B}$ is the flux density of the applied field (T) and $\overrightarrow{m}$ is the magnetization of the object (A/m). It is also possible to describe the applied magnetic field by the magnetic field intensity $\overrightarrow{H}$ (A/m), where $\overrightarrow{B} = \mu_0 \overrightarrow{H}$ and $\mu_0 = 4\pi \times 10^{-7}$ T · m/A is the permeability of the free space.

The magnetization of the object, which generally varies across the body, can be modeled as constant throughout the body with a value equal to the average magnetization. We often consider the total dipole moment $\overrightarrow{M}$ of a magnetic body, which is the product of the magnetic body volume and the average magnetization. The magnetic force and torque as a function of the dipole moment can be expressed as:

$$\overrightarrow{f_m} = (\overrightarrow{M} \cdot \bigtriangledown) \overrightarrow{B} \tag{3}$$

$$\overrightarrow{\tau_m} = \overrightarrow{M} \times \overrightarrow{B} \tag{4}$$

From the relationship, we get that the magnetic force is proportional to the gradient of the magnetic field, which is used to move the object in the field to local maximum, and the magnetic torque is proportional to the magnetic field, which acts to align the magnetization of an object with the field.

3. Magnetic Actuation Systems

Magnetic actuation systems are capable of generating a magnetic field gradient and/or uniform magnetic fields, which are classified into two main categories: electromagnetic systems or rotating permanent magnetic systems. We will discuss their advantages and applications in this section.

3.1. Electromagnetic Actuation Systems

Electromagnets can be easily and simultaneously controlled by electric currents. Uniform magnetic fields and uniform magnetic gradient fields can be generated by the specific configuration of electromagnets: Helmholtz and Maxwell coils. The motion of microrobots actuated by uniform magnetic

fields or uniform magnetic gradient fields can be predicted. The electromagnets can be combined with each other in order to generate more complicated magnetic fields.

A uniform magnetic field can be generated by a Helmholtz coil pair, which is made up of two identical circular coils aligned on the same axis and separated by a distance equal to the radius of the coil with identical currents passing in the same direction. Therefore, a 3D Helmholtz coil system consists of three orthogonally-arranged Helmholtz coil pairs, as shown in Figure 1a, which can generate a uniform rotating magnetic field $\mathbf{B}_{\perp\mathbf{n}}$ around any axis $\mathbf{n}$ in the 3D space by the modulation of currents passing through the coils, which can be expressed as [43]:

$$\mathbf{B}_{\perp\mathbf{n}}(t) = B_0 \cos(2\pi f t)\tilde{\mathbf{u}} + B_0 \cos(2\pi f t)\tilde{\mathbf{v}} \tag{5}$$

where B_0 is the magnetic flux density at the center of the Helmholtz coils, f is the rotational frequency and $(\tilde{\mathbf{u}}, \tilde{\mathbf{v}})$ are the basis vectors of the plane orthogonal to the axis $\mathbf{n}$. The 3D Helmholtz coils capable of generating uniform rotating magnetic field are widely used by many researchers to rotate helical propulsive swimming microrobots in 3D space [41,45–47]. Moreover, with the modulation of the currents passing through the coils, the Helmholtz coil setup can generate various magnetic fields adapted for the motion control of different microrobots: for example, a square wave oscillating magnetic field for actuating a jellyfish-like swimming microrobot [48], an on/off magnetic field for the motion control of flexible metal nanowire motors [49] or for a magnetic mite (MagMite) [50] and a conical magnetic field to decrease the off-axis motion of helical microrobots [51].

A Maxwell coil pair can generate a uniform-gradient magnetic field, with the coils separated by $\sqrt{3}$ times the radius and the current passing in the opposite direction. Yesin *et al.* [55] developed a combination of a coaxial pair of Helmholtz coils and Maxwell coils to control an elliptical-shaped microrobot . The combination of coils is mounted on a rotating stage, so that it can rotate around the workspace to control the orientation of the magnetic field. Therefore, the setup enables three DoF, including one DoF of rotation and two DoF of translation. The direction of the magnetic field is changed by the mechanical method, which is not simultaneous.

The combination with two pairs of Maxwell coils and two pairs of Helmholtz coils enables also a three DoF control of the microrobots with a simultaneous change of the magnetic direction controlled by currents [56,57]. The combination of electromagnetic coils allows a faster control of the system and reduces mechanical noises. However, as the electromagnetic coils are orthogonally arranged, the inner diameter of the outer coil pair should be greater than the outer diameter of the inner coil pair. Therefore, the combination of electromagnetic coils is less geometrically-compact and costs more energy.

Kim *et al.* [58] proposed an electromagnetic system consisting of two pairs of Helmholtz coils, which was capable of generating a uniform magnetic field, as well as a magnetic gradient simultaneously by superposing Helmholtz and anti-Helmholtz currents (equal currents in the opposite direction). Magnetic torques exerted on microrobots are induced by the Helmholtz currents, and magnetic forces exerted on microrobots are induced by the anti-Helmholtz currents. The magnetic torques and forces caused a controlled 2D motion of their microrobot (a permanent magnetic cube) in the horizontal plane. This electromagnetic system possesses two pairs of Maxwell coils less than the former one. Therefore, the system with two pairs of Helmholtz coils controlled by superposing Helmholtz and anti-Helmholtz currents takes less volume and has more energy efficiency. Indeed, the control is more complicated.

Apropos of reducing the outer volume of the electromagnetic systems, Jeon *et al.* [53] proposed two pairs of saddle-shaped coils with different geometrical parameters and current directions: one can generate uniform magnetic fields named uniform saddle coils; the other one can generate a magnetic field gradient named gradient saddle coils (Figure 1b). The saddle-shaped coils are geometrically compact. Therefore, they can be easily combined with a pair of circular coils to increase the DoF of control. For example, Go *et al.* [59] combined a pair of Helmholtz coils and a pair of uniform saddle coils, which can be rotated by a motor, in order to enable three DoF motion control. The main advantage of the systems with saddle-shaped coils is that the ratio of the workspace and the outer volume of the system is high.

In order to increase further the energy efficiency and DoF of the motion control, researchers use a combination of electromagnets with small diameters and iron cores, as shown in Figure 1c. Kummer *et al.* [35] designed an electromagnetic system consisting of eight electromagnets named OctoMag. The OctoMag system enables five DoF wireless magnetic control of a fully-untethered microrobot, including three DoF of translation (3T) and two DoF of rotation (2R). Similar to OctoMag, electromagnetic systems consisting of multiple independently-controlled electromagnets are widely used for magnetically-actuated microrobots, such as the MiniMag with eight electromagnets used by Schuerle *et al.* [60], a system with six electromagnets developed by Pawashe *et al.* [61], a system with eight electromagnets arranged in a different way used by Diller *et al.* [62] and And *et al.* [54] and a system with four electromagnets used by Khalil *et al.* [42]. These kinds of electromagnetic systems enable motion control with a high DoF. However, the workspace is restrictive compared to the volume of the whole system.

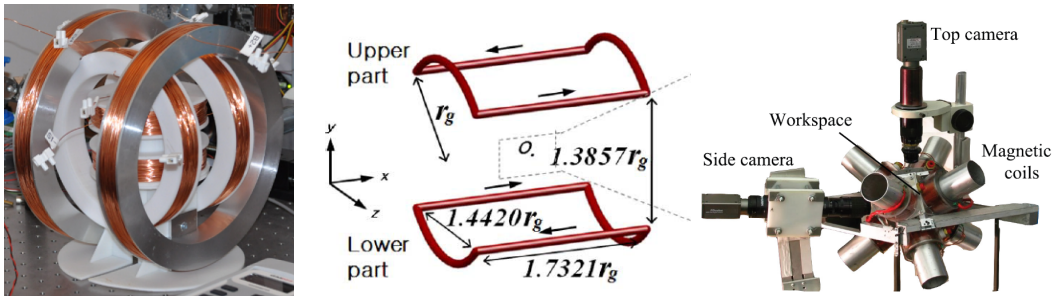

Figure 1. Electromagnetic systems: (**a**) 3D Helmholtz coils [52]; (**b**) gradient saddle-shaped coils (©2015 IEEE; reprinted, with permission from [53]); (**c**) electromagnetic system with eight electromagnets (©2015 Wiley; reprinted, with permission from [54]).

MRI systems provide a high homogeneous magnetic field and magnetic gradient, which benefit a larger workspace than any other electromagnetic system, but they are limited in DoF [31,63]. Hence, a robotic platform should be integrated in order to achieve 3D motion. Additionally, MRI systems are more often used for imaging purposes.

The electromagnetic actuation systems are summarized in Table 1 with their DoF and applications, and three different types are illustrated in Figure 1. Some of these are advantageous in high DoF motion control; some of them are advantageous in a large workspace. The choice of the electromagnetic system depends on the dimensions of the attempted motion control, the required workspace, the allowed maximal volume of the system and the power supply, which will be discussed in Section 5.

Table 1. Summary of electromagnetic actuation systems.

Scope	Composition	Application	DoF	Reference
Uniform field	3D Helmholtz coils	uniform rotating magnetic field	3 (3R)	[36,41,45,47]
		square wave oscillating field		[48]
		On/Off magnetic field		[49,50]
		conical magnetic field		[51]
Magnetic gradient	Uniform saddle coils	uniform magnetic field	1 (1R)	[53]
	OctoMag	motion control in 3D space	5 (2R + 3T)	[35]
	MiniMag	motion control in 3D space	5 (2R + 3T)	[60]
	Independently controlled electromagnets	motion control in 3D space	6 (3R + 3T)	[61,62]
Combined magnetic fields	Gradient saddle coils	Magnetic field gradient	1 (1T)	[53]
	One pair of Helmholtz coils + one pair of Maxwell coils + motorf	motion control in 2D plane	3 (1R + 2T)	[55]
	Two pairs of Helmholtz coils + two pairs of Maxwell coils	motion control in 2D plane	3 (1R + 2T)	[56,57]
	Two pairs of Helmholtz coils	motion control in 2D plane (Helmholtz currents $\geqslant$ torques + anti-Helmholtz currents $\geqslant$ forces)	3 (1R + 2T)	[58]
	One pair of Helmholtz coils + one pair of saddle coils + motor	motion control in 2D plane	3 (2R + 1T)	[59]

3.2. Rotating Permanent Magnetic Systems

As the electromagnetic systems are difficult to scale up due to the energy efficiency and cost, the actuation with a permanent magnet system can be considered as an alternative solution [64]. A rotating permanent magnet generates a periodic magnetic field at the position $\mathbf{p}$, which can be expressed as:

$$\mathbf{B}(\mathbf{p}, t + 2\pi f) = \mathbf{B}(\mathbf{p}, t) \tag{6}$$

where t is the time and f is the rotational frequency. The magnetic field can be accurately modeled with the point-dipole model [65]. The magnetic field $\mathbf{B}$ at a position $\mathbf{p}$ relative to the center of the permanent magnet can be expressed as follows:

$$\mathbf{B}(\mathbf{p}) = \frac{\mu}{4\pi|\mathbf{p}|^3}\left(\frac{3\mathbf{p}\mathbf{p}^T}{|\mathbf{p}|^2} - \mathbb{I}\right)\mathbf{M} \tag{7}$$

where μ is the permeability, $\mathbb{I}$ is the identity matrix and $\mathbf{M}$ is the dipole moment of the magnet, which is always perpendicular to the rotation axis. Mahoney *et al.* demonstrated that the magnetic field vector at every point in space, generated by a rotating magnetic dipole, such as a permanent magnet, rotates around a fixed axis [66]. The local field rotation axes for the axial and radial positions, which are defined respectively as the positions on the axis and the positions spanned by the rotating dipole, are parallel to

the rotation axis of the rotating dipole. Therefore, those positions have been used in many works for actuation due to their simplicity [64,67].

Many researchers used one single rotating permanent magnet to actuate their magnetic robots [64,67–70]. The rotating permanent magnet can be mounted on a linear stage [69] or a robotic arm [70] (Figure 2a), in order to increase the DoF of the system. The permanent magnetic systems are suitable for *in vivo* tasks, for which the applied organisms are too big for an electromagnetic system. For example, Mahoney *et al.* used a rotating permanent magnet mounted on a robotic arm to actuate an untethered magnetic device for the application in stomach capsule endoscopy [71]. The magnetic magnitude of a permanent magnet is stronger than electromagnets, but attenuates quickly with the distance. Therefore, the permanent magnet should approach the microrobots.

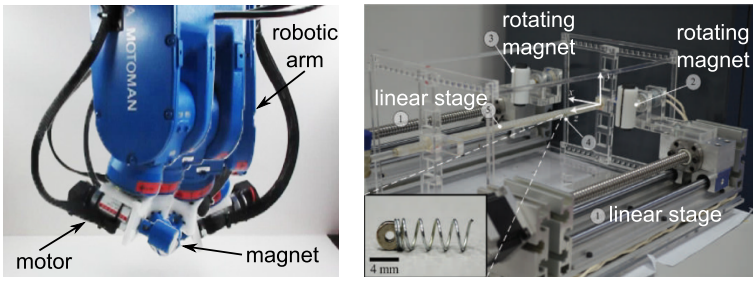

Figure 2. Rotating permanent magnetic systems: (**a**) a rotating permanent magnet mounted on a robotic arm (©2015 IEEE; reprinted, with permission from [70]); (**b**) two synchronized rotating permanent magnets mounted on two linear stages (©2015 IEEE; reprinted, with permission from [72]).

However, the single rotating permanent magnet provides undesirable magnetic force due to the magnetic gradient. In order to eliminate this undesirable lateral magnetic force, one can use two synchronized rotating permanent magnets system. Alshafeei *et al.* [72] demonstrated the motion control of magnetic helical swimming microrobots with two synchronized permanent magnets (Figure 2b). They showed that the lateral oscillations of the microrobots are decreased by using two synchronized permanent magnets. The radial steering of a helical swimming robot achieved higher motion stability.

Although the permanent magnetic systems are energy efficient and allow a large workspace, some disadvantages of the systems cannot be avoided. For example, the amplitude of the magnetic field cannot be changed easily. Furthermore, the magnetic field cannot be switched off, because of the permanent magnetic characteristics, which could cause safety problems. In addition, all of the changes of the magnetic field direction in a permanent magnetic system are realized by mechanical methods, which means that the changes are continuous and present mechanical noises. Therefore, it is impossible to generate a discontinuously-changed magnetic field, such as a square wave oscillating field. A benchmark on the choice of the magnetic actuating system will be discussed in Section 5.

4. Motion Control

This section describes the control methods for magnetically-actuated microrobots from open-loop control methods to closed-loop control methods. The open-loop control methods consist of two

categories: a pre-programmed control and an open-loop teleoperation. The closed-loop control methods include a point-to-point position control for holonomic mobile microrobots and a velocity-independent path following control for non-holonomic mobile microrobots. Current challenges in the motion control of microrobots will also be discussed.

4.1. Open-Loop Control

In order to realize a pre-programmed open-loop control, some control information should be estimated at first. For a microrobot pulled by a magnetic field gradient, Yesin *et al.* [55] estimates the necessary field gradient to resist fluid drag forces to actuate an elliptical microrobot. The microrobot is steered in the horizontal plane by a uniform magnetic field. As for helical swimmers actuated by a rotating magnetic field, researchers estimate the rotation direction of the field; for example, a rotating magnetic field with a fixed rotation axis to actuate the helical swimmer to follow a straight line [36,40,73]. Then, Ghosh *et al.* [37] achieved following a curved trajectory (e.g., "R@H") with their helical microrobots, which were navigated by a pre-programmed controller to actuate the magnetic field. Mahoney *et al.* [41] demonstrated a "U-turn" trajectory in a horizontal plane with the gravity compensation of helical microrobots. Jeong *et al.* [74] used a pair of Maxwell coils in the vertical direction to compensate the gravity of a drilling microrobot. The microrobot can be controlled to follow the predefined direction in a bifurcated tube, which mimics the blood vessels. Diller *et al.* [75] propelled a flexible sheet with magnetization varying along its length with a rotating magnetic field by forming continuous undulatory deformations. The undulatory swimming speed is a function of the magnetic field and frequency. This flexible microrobot can be driven along a predefined path. Nam *et al.* [76] developed a crawling microrobot, which can move along a tube by using the asymmetric friction force caused by an oscillating external magnetic field. The crawling microrobot can take the predefined direction in a bifurcated tube. The pre-programmed control of microrobots is summarized by a block-diagram, as shown in Figure 3. As there is no feedback in the control process, the microrobots are losing the reference trajectory or reference path, due to the presence of environment noises or boundary effects. To follow a reference trajectory means to follow a virtual robot in a time-dependent manner, and to follow a reference path means to follow a time-independent trajectory [77]. Note that sometimes, the errors of the swimming robots can be auto-corrected in a bifurcated tube by the presence of the tube wall, not by control methods. If the swimming robots are actuated in a free space (a water tank), they cannot go back to the reference path once losing it.

The microrobots capable of 3D steering are controlled using a classic open-loop teleoperation to transport cargos, demonstrated by Tottori *et al.* [78]. An open-loop teleoperation means that the users transmit only motion commands without any mechanical force feedback [79]. Visual feedback can be returned to the human operator without any tracking and calculation of the position of the microrobot. The block-diagram of open-loop teleoperation control method is described in Figure 4. With this control method, microrobots can correct the offtrack, but not in an automated manner. Therefore, this method can be applied on the targeted drug delivery task, which do not require high numbers of repetitions. However, the teleoperation is not suitable for the industrial tasks, which may require high repetitions with high precisions, for example the robotic micro-assembly processes.

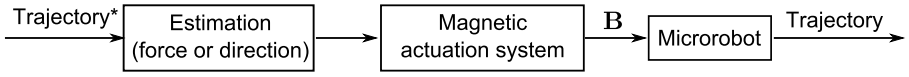

Figure 3. Block-diagram of the pre-programmed control of microrobots.

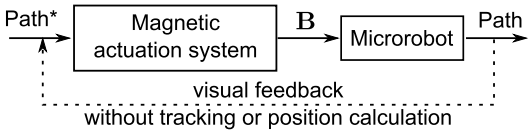

Figure 4. Block-diagram of open-loop teleoperation control of microrobots.

4.2. Closed-Loop Control

A closed-loop control of microrobots is necessary for precise motion in presence of perturbations generated by thermal noise [80], or drifting due to boundary effects [35,81,82]. A robust and efficient control system is required for microrobots, because the high sensitivity of the micro-systems to environmental variables, and the high velocities at the microscale. On-board sensors are hard to achieve due to the small scale. A fast external sensing method is thus required to locate the microrobots, such as vision.

For an elliptic microrobot, which can move from one location to another in a holonomic way, Kummer *et al.* [35] implemented a simple proportional-derivative (PD) controller to estimated the magnetic forces based on the error of the position. For a desired magnetic force, the current can be computed for each coil. The real-time 3D position of the microrobot is based on the tracking scheme using the adaptive thresholding and morphological operators, such as erosion and dilation. Nevertheless, the orientation of the microrobot is controlled by an open-loop method. The Block-diagram of the closed-loop positioning control of this holonomic microrobot is shown in Figure 5. This kind of point-to-point closed-loop position control is widely used for holonomic mobile microrobots. Pawashe *et al.* [83] achieved the visual servoing of the magnetic microrobot (Mag-μBots) by a basic proportional-integral (PI) controller, which aims to reduce the error between the microrobot and its target position by varying its velocity. The Mag-μBots are actuated by using oscillating magnetic fields, which results in stick-slip motion on a 2D surface. Zhang *et al.* [84] demonstrated a visual servo control of a magnetic bead actuated by a magnetic gradient, using a model-based nonlinear control law, combining feedback linearization and minimum variance control. The magnetic bead is capable of stable positioning in 3D.

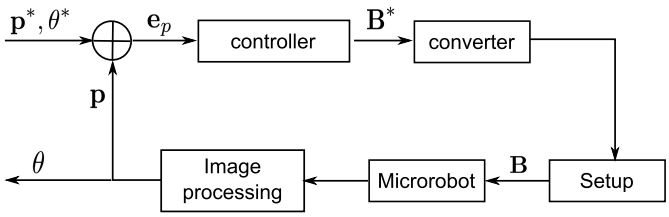

Figure 5. Block-diagram of the control of a holonomic microrobot. Notations: $\mathbf{p}$ and $\mathbf{p}^*$ are respectively the real-time and target position of the microrobot; θ and θ^* are respectively the real-time and target orientation of the microrobot; $\mathbf{e}_p$ is the error of the position; $\mathbf{B}$ and $\mathbf{B}^*$ are respectively the generated and the calculated magnetic field to control the microrobot.

For a non-holonomic mobile microrobot, such as a helical swimming microrobot, someone cannot apply a simple proportional-integral-derivative (PID) controller on the position of the microrobot, because a non-holonomic system is a mechanical system with constraints on the velocity that are not derivable for position constraints [85]. Therefore, Xu *et al.* [43] developed a velocity-independent control law of the helical system to follow a planar reference path based on a 3D steering, because it is indeed very delicate to follow a time-dependent trajectory (e.g., to follow a virtual robot) in the presence of thermal noise, because thermal noise will yield time delays with the virtual robot on the trajectory, and thus, the geometrical path will not be achieved. As presented by the block-diagram of the 2D path following control in Figure 6, two controllers are implemented in the control. The first controller, Controller I, is inspired by the path following of a unicycle mobile robot [77,86] to minimize the lateral error, which deduces the target orientation of the helical swimmer. The second controller, Controller II, is a P controller based on the orientation error of the helical swimmer in the 3D space, which gives the target actuating magnetic field. Another kind of non-holonomic mobile microrobot is a rolling magnetic microrobot, which can generate a forward velocity on a surface induced by a rolling motion actuated by a rotating magnetic field. Kim *et al.* [87] controlled a rolling spherical magnetic microrobot to follow a pre-defined spiral path. Pieters *et al.* [88] controlled a rolling rod-shaped microrobot to follow a virtual target on a reference path, which is inspired by the trajectory following the control laws of unicycles. The controllers are similar to Controller I in Figure 6. The autonomous closed-loop control of microrobots can be applied to micro-manipulation, including trapping, sorting and transportation of micro-objects and assembly of multiple micro-objects.

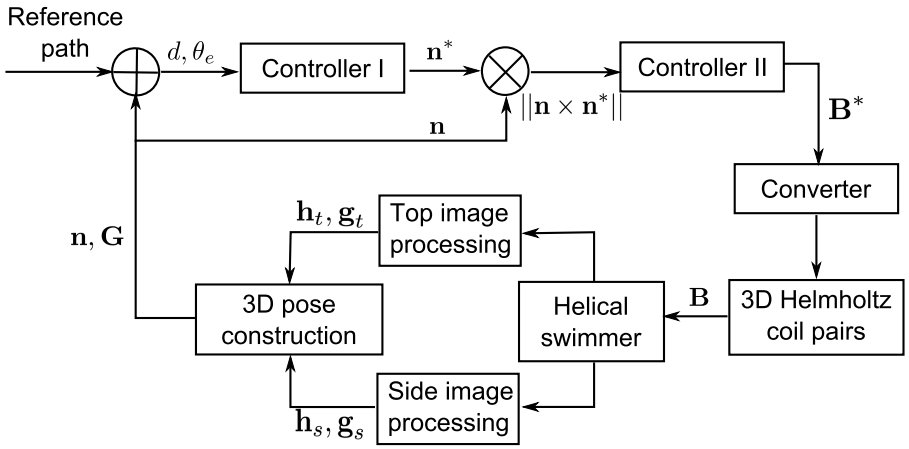

Figure 6. Block-diagram of the control of a non-holonomic helical swimmer for planar path following. Controller I: linearization of the state-space model of the helical swimmer for path following with chained forms. Controller II: P controller for 3D steering. Notations: d is the lateral error between the helical swimmer and the path; θ_e is the angle error between the orientation of the swimmer and the tangent of the path; $\mathbf{n}$ and $\mathbf{n}^*$ are respectively the real-time and the target orientation of the helical swimmer in the 3D space; $\mathbf{h}_\mathrm{t}$ and $\mathbf{h}_\mathrm{s}$ are respectively the tracked axis of the swimmer in the top and side camera image; $\mathbf{g}_\mathrm{t}$ and $\mathbf{g}_\mathrm{s}$ are respectively the tracked barycenter of the swimmer in the top and side camera image; $\mathbf{G}$ is the calculated barycenter of the swimmer in the 3D space.

The magnetic actuation-based motion control of microrobots is summarized in Table 2. A benchmark on the choice of the motion control method will be discussed and concluded in Section 5.

Table 2. Summary of magnetic actuation based motion control methods of microrobots.

Microrobots	Actuation	Control	Reference
Holonomic	Pulling by magnetic gradient	Pre-programmed open-loop control	[55]
		Point to point closed-loop position control	[35,84]
	Stick-slip motion by oscillating fields	Point to point closed-loop position control	[83]
Non-holonomic	Helical propulsion by rotating fields	Pre-programmed open-loop control	[36,37,73]
		Open-loop teleoperation	[78]
		Closed-loop planar path following	[43]
	Drilling by rotating fields and pulling by gradient	Pre-programmed open-loop control	[74]
	Undulatory swimming	Pre-programmed open-loop control	[75]
	Clawing motion by oscillating fields	Pre-programmed open-loop control	[76]
	Rolling motion by rotating fields	Closed-loop planar path following	[87]
		Closed-loop planar trajectory following	[88]

4.3. Challenges in Motion Control of Microrobots

Simultaneous control of multiple untethered magnetic microrobots is a significant challenge in motion control of microrobots. Kratochvil *et al.* [89] demonstrated the individual control of two microrobots with different resonant frequencies. The responses of these individual microrobots to the global driving magnetic field differ achieves the appearance of simultaneous motion control. Diller *et al.* [90] fabricated geometrically-dissimilar microrobots (Mag-μBots), which were actuated by a stick-slip motion and responded differently to the actuation magnetic fields. The Mag-μBots can be controlled in a coupled fashion that allows for independent global positioning of each microrobot. The motion control was shown in two dimensions. Later, Diller *et al.* [62] demonstrated a new method to independently control multiple microrobots in three dimensions by using magnetic gradient pulling forces. The independent control is based on the difference of the geometry and magnetization of microrobots. Therefore, increasing the limit of the independent control requires reducing the coupling of microrobots.

5. Discussions and Conclusions

In this paper, we have reviewed the magnetic actuation systems, including electromagnetic systems and permanent magnetic systems. The electromagnetic coils can be combined easily with each other in order to generate complicated magnetic fields. The electromagnetic coils can also be combined with a mechanical structure, usually a rotational motor, to generate rotating fields. In this case, the change of magnetic field direction cannot be discontinuous, such as an on/off magnetic field or a square wave oscillating field. Therefore, if discontinuously-changed magnetic fields are required for the microrobot actuation, a pure electromagnetic system should be used. The required DoF of the motion control in applications can define the design of the arrangement of the electromagnetic coils. Most electromagnetic systems benefit from a high DoF, but only allow a relatively restrictive workspace. These magnetic

actuation systems are suitable for the applications of microrobots in micro-channels or labs-on-chips. The energy cost increases dramatically with the dimension of the electromagnetic coils, and the energy efficiency decreases. Permanent magnetic systems can be alternative solutions. Permanent magnets are mounted on mechanical structures, such as robotic arms or linear stages, to generate alternating magnetic fields. The permanent magnetic systems are suitable for some simple *in vivo* tasks, for example actuating a microrobot in human arms, for which the applied organisms are too big for an electromagnetic system. Some disadvantages cannot be avoided, such as the magnetic field cannot be switched off, and it is hard to achieve alternating fields with high frequency. The benchmark of the magnetic actuation systems is shown in Figure 7. Once the actuation system is chosen, for future studies, the parameters of the system (combination of coils, geometrical parameters, current, *etc*.) should be optimized according to the requirement of the application (magnetic fields strength, DoF, workspace, *etc*.), in order to maximize the energy efficiency of the system and to improve the performance of the microrobots [91].

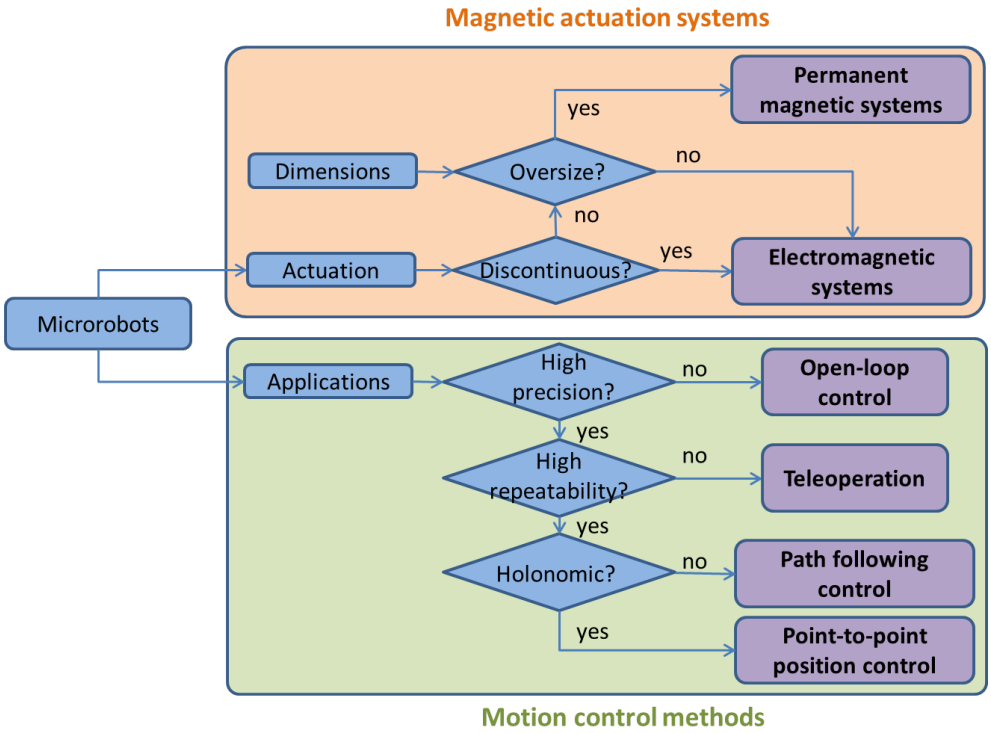

Figure 7. An overall benchmark on the magnetic actuation systems and motion control methods.

We have also reviewed the magnetic actuation-based control methods and have summarized with block-diagrams in this paper. Researchers have historically used an open-loop pre-programmed control method at the early stage to characterize the microrobots, which does not require high precision control. However, for many applications, the correction of path or position error is required due to the presence of environmental noises. The teleoperation method can be applied to the transportation tasks without a high number of repetitions, for example targeted drug delivery, or manipulation, which requires interaction with the manipulators, for example the selection of micro-objects. For industrial micro-assembly or operations with many repetitions, autonomous closed-loop control methods with high precisions are required. A simple PD controller can be applied for a point-to-point 3D position control of holonomic

microrobots. As for a non-holonomic mobile microrobot, such as a helical swimming microrobot, researchers have developed a velocity-independent control law to follow a planar reference path. The path following control of microrobots can achieve complicated tasks, for example cell surgery and surgery in blood vessels. The benchmark of the magnetic actuation-based motion control methods is depicted in Figure 7.

For future research of the magnetic actuation-based control of microrobots, closed-loop control for non-holonomic mobile microrobots in 3D space should be investigated. The independent control of a microrobot in a group of multiple magnetic microrobots and the swarm control of a group of magnetic microrobots are also challenging in the motion control of microrobots. Researchers could also continue the research on the integration of other sensing methods, such as fluoroscopy, CT and X-ray, instead of vision in the control systems, in order to track the microrobots for *in vivo* applications.

Acknowledgments

This work was partially supported by the early career scheme (ECS) grant with Project No. 439113 and the General Research Fund (GRF) with Project No. 417812 from the Research Grants Council (RGC) of Hong Kong SAR, the National Natural Science Funds of China for Young Scholar with the Project No. 61305124 and the grant from the Science, Technology and Innovation Committee of Shenzhen Municipality (SZSTI) for the Basic Research Fund with Project No. JCYJ20140905151415999. This work was also partially supported by the Korea Evaluation Institute of Industrial Technology (KEIT) funded by the Ministry of Trade, Industry & Energy (No. 10052980).

Author Contributions

Tiantian Xu made the main contribution on literature review and led the development of the paper. Jiangfan Yu, Xiaohui Yan, Hongsoo Choi and Li Zhang performed supports and discussions. All authors reviewed and approved the submitted paper.

Conflicts of Interest

The authors declare no conflict of interest.

References

1. Abbott, J.; Nagy, Z.; Beyeler, F.; Nelson, B. Robotics in the Small, Part I: Microbotics. *IEEE Rob. Autom Mag.* **2007**, *14*, 92–103.
2. Abbott, J.; Cosentino Lagomarsino, M.; Zhang, L.; Dong, L.; Nelson, B. How Should Microrobots Swim? *Int. J. Rob. Res.* **2009**, *28*, 1434–1447.
3. Sitti, M. Miniature devices: Voyage of the microrobots. *Nature* **2009**, *458*, 1121–1122.
4. Nelson, B.; Kaliakatsos, I.; Abbott, J. Microrobots for Minimally Invasive Medicine. *Annu. Rev. Biomed. Eng.* **2010**, *12*, 55–85.
5. Gauthier, M.; Régnier, S. *Robotic Micro-Assembly*; IEEE Press: Piscataway, NJ, USA, 2010.

6. Qiu, F.; Zhang, L.; Tottori, S.; Marquardt, K.; Krawczyk, K.; Franco-Obregón, A.; Nelson, B.J. Bio-inspired microrobots. *Mater. Today* **2012**, *15*, 463.
7. Chaillet, N.; Régnier, S. *Microrobotics for Micromanipulation*; Wiley-ISTE: Hoboken, NJ, USA, 2013.
8. Peyer, K.; Zhang, L.; Nelson, B. Bio-inspired magnetic swimming microrobots for biomedical applications. *Nanoscale* **2013**, *5*, 1259–1272.
9. Sitti, M.; Ceylan, H.; Hu, W.; Giltinan, J.; Turan, M.; Yim, S.; Diller, E. Biomedical Applications of Untethered Mobile Milli/Microrobots. *Proc. IEEE* **2015**, *103*, 205–224.
10. Ferreira, A.; Cassier, C.; Hirai, S. Automatic microassembly system assisted by vision servoing and virtual reality. *IEEE/ASME Trans. Mechatron.* **2004**, *9*, 321–333.
11. Xie, H.; Régnier, S. High-efficiency automated nanomanipulation with parallel imaging/manipulation force microscopy. *IEEE Trans. Nanotechnol.* **2012**, *11*, 21–33.
12. Bolopion, A.; Xie, H.; Haliyo, S.; Régnier, S. Haptic Teleoperation for 3D Microassembly of Spherical Objects. *IEEE/ASME Trans. Mechatron.* **2012**, *17*, 116–127.
13. Fukuda, T.; Ueyama, T. *Cellular Robotics and Micro Robotic Systems*; World Scientific: Singapore, 1994; Voloum 10.
14. Truper, T.; Kortschack, A.; Jahnisch, M.; Hulsen, H.; Fatikow, S. Transporting cells with mobile microrobots. *IET Proc. Nanobiotechnol.* **2004**, *151*, 145–150.
15. Suter, M.; Zhang, L.; Siringil, E.C.; Peters, C.; Luehmann, T.; Ergeneman, O.; Peyer, K.E.; Nelson, B.J.; Hierold, C. Superparamagnetic microrobots: Fabrication by two-photon polymerization and biocompatibility. *Biomed. Microdevices* **2013**, *15*, 997–1003.
16. Feng, L.; Hagiwara, M.; Uvet, H.; Yamanish, Y.; Kawahara, T.; Kosuge, K.; Arai, F. High-speed delivery of microbeads in microchannel using magnetically driven microtool. In Proceedings of the 16th International Conference on Solid-State Sensors, Actuators and Microsystems (TRANSDUCERS), Beijing, China, 5–9 June 2011; pp. 1312–1315.
17. Hagiwara, M.; Kawahara, T.; Iijima, T.; Yamanishi, Y.; Arai, F. High speed microrobot actuation in a microfluidic chip by levitated structure with riblet surface. In Proceedings of the IEEE International Conference on Robotics and Automation (ICRA), St. Paul, MN, USA, 14–18 May 2012; pp. 2517–2522.
18. Hagiwara, M.; Kawahara, T.; Iijima, T.; Arai, F. High-Speed Magnetic Microrobot Actuation in a Microfluidic Chip by a Fine V-Groove Surface. *IEEE Trans. Rob.* **2013**, *29*, 363–372.
19. Sanchez, S.; Solovev, A.; Harazim, S.; Schmidt, O. Microbots Swimming in the Flowing Streams of Microfluidic Channels. *J. Am. Chem. Soc.* **2011**, *133*, 701–703.
20. Hwang, G.; Ivan, I.A.; Agnus, J.; Salmon, H.; Alvo, S.; Chaillet, N.; Régnier, S.; Haghiri-Gosnet, A.M. Mobile microrobotic manipulator in microfluidics. *Sens. Actuators A Phys.* **2013**, *215*, 56–64.
21. Gao, W.; Wang, J. The environmental impact of micro/nanomachines: A review. *ACS Nano* **2014**, *8*, 3170–3180.
22. Kim, S.; Qiu, F.; Kim, S.; Ghanbari, A.; Moon, C.; Zhang, L.; Nelson, B.J.; Choi, H. Fabrication and Characterization of Magnetic Microrobots for Three-Dimensional Cell Culture and Targeted Transportation. *Adv. Mater.* **2013**, *25*, 5863–5868.
23. Peyer, K.; Siringil, E.; Zhang, L.; Nelson, B. Magnetic polymer composite artificial bacterial flagella. *Bioinspiration Biomim.* **2014**, *9*, 046014.

24. Zhang, L.; Petit, T.; Peyer, K.E.; Nelson, B.J. Targeted cargo delivery using a rotating nickel nanowire. *Nanomed. Nanotechnol. Biol. Med.* **2012**, *8*, 1074–1080.
25. Yan, X.; Zhou, Q.; Yu, J.; Xu, T.; Yan, D.; Tang, T.; Feng, Q.; Bian, L.; Zhang, Y.; Ferreira, A.; Zhang, L. Magnetite Nanostructured Porous Hollow Helical Microswimmers for Targeted Delivery. *Adv. Funct. Mater.* **2015**, *25*, 5333–5342.
26. Kharboutly, M.; Gauthier, M.; Chaillet, N. Modeling the Trajectory of a Microparticle in a Dielectrophoresis Device. *J. Appl. Phys.* **2009**, *106*, 114312–114317.
27. Kosa, G.; Shoham, M.; Zaaroor, M. Propulsion Method for Swimming Microrobots. *IEEE Trans. Rob.* **2007**, *23*, 137–150.
28. Liew, L.A.; Bright, V.M.; Dunn, M.L.; Daily, J.W.; Raj, R. Development of SiCN ceramic thermal actuators. In Proceedings of the 15th IEEE International Conference on Micro Electro Mechanical Systems, Las Vegas, NV, USA, 20–24 January 2002; pp. 590–593.
29. Hwang, G.; Braive, R.; Couraud, L.; Cavanna, A.; Abdelkarim, O.; Robert-Philip, I.; Beveratos, A.; Sagnes, I.; Haliyo, S.; Régnier, S. Electro-osmotic propulsion of helical nanobelt swimmers. *Int. J. Rob. Res.* **2011**, *30*, 806–819.
30. Martel, S.; Tremblay, C.C.; Ngakeng, S.; Langlois, G. Controlled manipulation and actuation of micro-objects with magnetotactic bacteria. *Appl. Phys. Lett.* **2006**, *89*, 233904.
31. Martel, S.; Felfoul, O.; Mathieu, J.B.; Chanu, A.; Tamaz, S.; Mohammadi, M.; Mankiewicz, M.; Tabatabaei, N. MRI-based medical nanorobotic platform for the control of magnetic nanoparticles and flagellated bacteria for target interventions in human capillaries. *Int. J. Rob. Res.* **2009**, *28*, 1169–1182.
32. Solovev, A.A.; Mei, Y.; Bermúdez Ureña, E.; Huang, G.; Schmidt, O.G. Catalytic Microtubular Jet Engines Self-Propelled by Accumulated Gas Bubbles. *Small* **2009**, *5*, 1688–1692.
33. Gao, W.; Pei, A.; Wang, J. Water-driven micromotors. *ACS Nano* **2012**, *6*, 8432–8438.
34. Fahrni, F.; Prins, M.W.; Van IJzendoorn, L.J. Micro-fluidic actuation using magnetic artificial cilia. *Lab Chip* **2009**, *9*, 3413–3421.
35. Kummer, M.; Abbott, J.; Kratochvil, B.; Borer, R.; Sengul, A.; Nelson, B. OctoMag: An electromagnetic system for 5-DOF wireless micromanipulation. *IEEE Trans. Rob.* **2010**, *26*, 1006–1017.
36. Zhang, L.; Abbott, J.; Dong, L.; Kratochvil, B.; Bell, D.; Nelson, B. Artificial bacterial flagella: Fabrication and magnetic control. *Appl. Phys. Lett.* **2009**, *94*, 064107.
37. Ghosh, A.; Fischer, P. Controlled Propulsion of Artificial Magnetic Nanostructured Propellers. *Nano Lett.* **2009**, *9*, 2243–2245.
38. Peyer, K.E.; Tottori, S.; Qiu, F.; Zhang, L.; Nelson, B.J. Magnetic helical micromachines. *Chem. Eur. J.* **2013**, *19*, 28–38.
39. Xu, T.; Hwang, G.; Andreff, N.; Regnier, S. Modeling and Swimming Property Characterizations of Scaled-Up Helical Microswimmers. *IEEE/ASME Trans. Mechatron.* **2014**, *19*, 1069–1079.
40. Ishiyama, K.; Arai, K.; Sendoh, M.; Yamazaki, A. Spiral-type micro-machine for medical applications. In Proceedings of the International Symposium onMicromechatronics and Human Science (MHS), Nagoya, Japan, 22–25 October 2000; pp. 65–69.
41. Mahoney, A.; Sarrazin, J.; Bamberg, E.; Abbott, J. Velocity Control with Gravity Compensation for Magnetic Helical Microswimmers. *Adv. Rob.* **2011**, *25*, 1007–1028.

42. Khalil, I.; Pichel, M.; Abelmann, L.; Misra, S. Closed-loop control of magnetotactic bacteria. *Int. J. Rob. Res.* **2013**, *32*, 637–649.
43. Xu, T.; Hwang, G.; Andreff, N.; Regnier, S. Planar Path Following of 3-D Steering Scaled-Up Helical Microswimmers. *IEEE Trans. Rob.* **2015**, *31*, 117–127.
44. Jiles, D. *Introduction to Magnetism and Magnetic Materials*, 2nd ed.; Chapman and Hall: Boca Raton, FL, USA, 1998.
45. Sendoh, M.; Yamazaki, A.; Chiba, A.; Soma, M.; Ishiyama, K.; Arai, K. Spiral type magnetic micro actuators for medical applications. In *Micro-Nanomechatronics and Human Science*, Proceedings of the 4th IEEE International Symposium on Symposium Micro-Nanomechatronics for Information-Based Society, Iijima, Japen, 31 October–3 November 2004; pp. 319–324.
46. Zhang, L.; Peyer, K.; Nelson, B. Artificial bacterial flagella for micromanipulation. *Lab Chip* **2010**, *10*, 2203–2215.
47. Xu, T.; Hwang, G.; Andreff, N.; Régnier, S. Characterization of Three-dimensional Steering for Helical Swimmers. In Proceedings of the ICRA'14 IEEE International Conference on Robotics and Automation, Hong Kong, China, 31 May–7 June 2014; pp. 4045–4051.
48. Ko, Y.; Na, S.; Lee, Y.; Cha, K.; Ko, S.; Park, J.; Park, S. A jellyfish-like swimming mini-robot actuated by an electromagnetic actuation system. *Smart Mater. Struct.* **2012**, *21*, 057001.
49. Gao, W.; Sattayasamitsathit, S.; Manesh, K.; Weihs, D.; Wang, J. Magnetically powered flexible metal nanowire motors. *J. Am. Chem. Soc.* **2010**, *132*, 14403–14405.
50. Frutiger, D.R.; Vollmers, K.; Kratochvil, B.E.; Nelson, B.J. Small, fast, and under control: Wireless resonant magnetic micro-agents. *Int. J. Rob. Res.* **2010**, *29*, 613–636.
51. Huang, T.; Qiu, F.; Tung, H.; Chen, X.; Nelson, B.; Sakar, M. Generating mobile fluidic traps for selective three-dimensional transport of microobjects. *Appl. Phys. Lett.* **2014**, *105*, 114102.
52. Xu, T. Propulsion Characteristics and Visual Servo Control of Scaled-up Helical Microswimmers. Ph.D. Thesis, The Université Pierre et Marie Curie-Paris VI, Paris, France, 2014.
53. Jeon, S.; Jang, G.; Choi, H.; Park, S. Magnetic navigation system with gradient and uniform saddle coils for the wireless manipulation of micro-robots in human blood vessels. *IEEE Trans. Magn.* **2010**, *46*, 1943–1946.
54. And, E.D.; Sitti, M. Three-Dimensional Programmable Assembly by Untethered Magnetic Robotic Micro-Grippers. *Adv. Funct. Mater.* **2014**, *24*, 4397–4404.
55. Yesin, K.; Vollmers, K.; Nelson, B. Modeling and control of Untethered Biomicrorobots in a Fluidic environment using Electromagnetic Fields. *Int. J. Rob. Res.* **2006**, *25*, 527–536.
56. Choi, J.; Choi, H.; Cha, K.; Park, J.O.; Park, S. Two-dimensional locomotive permanent magnet using electromagnetic actuation system with two pairs stationary coils. In Proceedings of the IEEE International Conference on IEEE Robotics and Biomimetics (ROBIO), Guilin, China, 13–19 December 2009; pp. 1166–1171.
57. Hu, C.; Tercero, C.; Ikeda, S.; Fukuda, T.; Arai, F.; Negoro, M. Modeling and design of magnetic sugar particles manipulation system for fabrication of vascular scaffold. In Proceedings of the IEEE/RSJ International Conference on IEEE Intelligent Robots and Systems (IROS), San Francisco, CA, USA, 25–30 September 2011; pp. 439–444.

58. Kim, J.; Kim, M.; Yoo, J.; Kim, S.J. Novel Motion Modes for 2-D Locomotion of a Microrobot. *IEEE Trans. Magn.* **2014**, *50*, 1–5.
59. Go, G.; Choi, H.; Jeong, S.; Lee, C.; Ko, S.Y.; Park, J.O.; Park, S. Electromagnetic Navigation System Using Simple Coil Structure (4 Coils) for 3-D Locomotive Microrobot. *IEEE Trans. Magn.* **2015**, *51*, 1–7.
60. Schuerle, S.; Erni, S.; Flink, M.; Kratochvil, B.E.; Nelson, B.J. Three-Dimensional Magnetic Manipulation of Micro- and Nanostructures for Applications in Life Sciences. *IEEE Trans. Magn.* **2013**, *49*, 321–330.
61. Pawashe, C.; Floyd, S.; Sitti, M. Modeling and experimental characterization of an untethered magnetic micro-robot. *Int. J. Rob. Res.* **2009**, *28*, 1077–1094.
62. Diller, E.; Giltinan, J.; Sitti, M. Independent control of multiple magnetic microrobots in three dimensions. *Int. J. Rob. Res.* **2013**, *32*, 614–631.
63. Vartholomeos, P.; Fruchard, M.; Ferreira, A.; Mavroidis, C. MRI-guided nanorobotic systems for therapeutic and diagnostic applications. *Annu. Rev. Biomed. Eng.* **2011**, *13*, 157–184.
64. Fountain, T.; Kailat, P.; Abbott, J. Wireless control of magnetic helical microrobots using a rotating-permanent-magnet manipulator. In Proceedings of the IEEE International Conference on Robotics and Automation (ICRA), Anchorage, AK, USA, 3–7 May 2010; pp. 576–581.
65. Furlani, E. *Permanent Magnet and Electromechanical Devices: Materials, Analysis, and Applications*; Electromagnetism, Elsevier Science: Amsterdam, The Netherlands, 2001.
66. Mahoney, A.; Cowan, D.; Miller, K.; Abbott, J. *Control of Untethered Magnetically Actuated Tools Using a Rotating Permanent Magnet in Any Position*; IEEE Press: Piscataway, NJ, USA, 2012; pp. 3375–3380.
67. Mahoney, A.; Abbott, J. Control of untethered magnetically actuated tools with localization uncertainty using a rotating permanent magnet. In Proceedings of the 4th IEEE RAS EMBS International Conference on Biomedical Robotics and Biomechatronics (BioRob), Rome, Italy, 24–27 June 2012; pp. 1632 –1637.
68. Lee, J.; Kim, B.; Hong, Y. A flexible chain-based screw propeller for capsule endoscopes. *Int. J. Precis. Eng. Manuf.* **2009**, *10*, 27–34.
69. Xu, T.; Hwang, G.; Andreff, N.; Régnier, S. Scaled-Up Helical Nanobelt Modeling and Simulation at Low Reynolds Numbers. In Proceedings of the ICRA'12 IEEE International Conference on Robotics and Automation, St. Paul, MN, USA, 14–18 May 2012; pp. 4045–4051.
70. Mahoney, A.W.; Abbott, J.J. Generating Rotating Magnetic Fields with a Single Permanent Magnet for Propulsion of Untethered Magnetic Devices in a Lumen. *IEEE Trans. Rob.* **2014**, *30*, 411–420.
71. Mahoney, A.; Abbott, J. Five-degree-of-freedom Manipulation of an Untethered Magnetic Device in Fluid Using a Single Permanent Magnet with Application in Stomach Capsule Endoscopy. *Int. J. Rob. Res.* **2015**, doi:10.1177/0278364914558006.
72. Alshafeei, M.; Hosney, A.; Klingner, A.; Misra, S.; Khalil, I.S. Magnetic-based motion control of a helical robot using two synchronized rotating dipole fields. In Proceedings of the 5th IEEE RAS EMBS International Conference on Biomedical Robotics and Biomechatronics, Sao Paulo, Brazil, 12–15 August 2014; pp. 151–156.

73. Zhang, L.; Abbott, J.; Dong, L.; Peyer, K.; Kratochvil, B.; Zhang, H.; Bergeles, C.; Nelson, B.J. Characterizing the Swimming Properties of Artificial Bacterial Flagella. *Nano Lett.* **2009**, *9*, 3663–3667.
74. Jeong, S.; Choi, H.; Cha, K.; Li, J.; Park, J.O.; Park, S. Enhanced locomotive and drilling microrobot using precessional and gradient magnetic field. *Sens. Actuators A Phys.* **2011**, *171*, 429–435.
75. Diller, E.; Zhuang, J.; Lum, G.Z.; Edwards, M.R.; Sitti, M. Continuously distributed magnetization profile for millimeter-scale elastomeric undulatory swimming. *Appl. Phys. Lett.* **2014**, *104*, 174101.
76. Nam, J.; Jeon, S.; Kim, S.; Jang, G. Crawling microrobot actuated by a magnetic navigation system in tubular environments. *Sens. Actuators A Phys.* **2014**, *209*, 100–106.
77. Laumond, J. (Ed.) *La Robotique Mobile*; Traité IC2, Hermés science: Paris, France, 2001.
78. Tottori, S.; Zhang, L.; Qiu, F.; Krawczyk, K.; Franco-Obregon, A.; Nelson, B. Magnetic Helical Micromachines: Fabrication, Controlled Swimming, and Cargo Transport. *Adv. Mater.* **2012**, *24*, 811–816.
79. Shull, P.; Niemeyer, G. Open-loop bilateral teleoperation for stable force tracking. In Proceedings of the IEEE/RSJ International Conference on Intelligent Robots and Systems (IROS), St. Louis, MO, USA, 11–15 October 2009; pp. 5121–5126.
80. Ghosh, A.; Paria, D.; Rangarajan, G.; Ghosh, A. Velocity Fluctuations in Helical Propulsion: How Small Can a Propeller Be. *J. Phys. Chem. Lett.* **2014**, *5*, 62–68.
81. Peyer, K.; Zhang, L.; Kratochvil, B.; Nelson, B. Non-ideal swimming of artificial bacterial flagella near a surface. In Proceedings of the 2010 IEEE International Conference on Robotics and Automation (ICRA), Anchorage, AK, USA, 3–7 May 2010; pp. 96–101.
82. Mahoney, A.; Nelson, N.; Parsons, E.; Abbott, J. Non-ideal behaviors of magnetically driven screws in soft tissue. In Proceedings of the IEEE/RSJ International Conference on IEEE Intelligent Robots and Systems (IROS), Vilamoura-Algarve, Portugal, 7–11 October 2012; pp. 3559–3564.
83. Pawashe, C.; Floyd, S.; Diller, E.; Sitti, M. Two-dimensional autonomous microparticle manipulation strategies for magnetic microrobots in fluidic environments. *IEEE Trans. Rob.* **2012**, *28*, 467–477.
84. Zhang, Z.; Long, F.; Menq, C. Three-Dimensional Visual Servo Control of a Magnetically Propelled Microscopic Bead. *IEEE Trans. Rob.* **2013**, *29*, 373–382.
85. Bloch, A.; Marsden, J.; Zenkov, D. Nonholonomic Dynamics. *Not. AMS* **2005**, *52*, 320–329.
86. Thuilot, B.; Cariou, C.; Martinet, P.; Berducat, M. Automatic Guidance of a Farm Tractor Relying on a Single CP-DGPS. *Auton. Rob.* **2002**, *13*, 53–71.
87. Kim, S.J.; Jeon, S.M.; Nam, J.K.; Jang, G.H. Closed-Loop Control of a Self-Positioning and Rolling Magnetic Microrobot on 3D Thin Surfaces Using Biplane Imaging. *IEEE Trans. Magn.* **2014**, *50*, 1–4.
88. Pieters, R.; Tung, H.W.; Charreyron, S.; Sargent, D.F.; Nelson, B.J. RodBot: A rolling microrobot for micromanipulation. In Proceedings of the IEEE International Conference on IEEE Robotics and Automation (ICRA), Seattle, WA, USA, 26–30 May 2015; pp. 4042–4047.

89. Kratochvil, B.E.; Frutiger, D.; Vollmers, K.; Nelson, B.J. Visual servoing and characterization of resonant magnetic actuators for decoupled locomotion of multiple untethered mobile microrobots. In Proceedings of the IEEE Robotics and Automation (ICRA'09), Kobe, Japan, 9 May 2009; pp. 1010–1015.
90. Diller, E.; Floyd, S.; Pawashe, C.; Sitti, M. Control of multiple heterogeneous magnetic microrobots in two dimensions on nonspecialized surfaces. *IEEE Trans. Rob.* **2012**, *28*, 172–182.
91. Erni, S.; Schürle, S.; Fakhraee, A.; Kratochvil, B.E.; Nelson, B.J. Comparison, optimization, and limitations of magnetic manipulation systems. *J. Micro-Bio Rob.* **2013**, *8*, 107–120.